Star Polymers in Shear Flow

M. Ripoll,* R. G. Winkler, and G. Gompper
Institut für Festkörperforschung, Forschungszentrum Jülich, D-52425 Jülich, Germany
(Received 27 January 2006; published 11 May 2006)

Linear and star polymers in solution are studied in the presence of shear flow. The solvent is described by a particle-based mesoscopic simulation technique, which accounts for hydrodynamic interactions. The scaling properties of the average gyration tensor, the orientation angle, and the rotation frequency are investigated for various arm lengths and arm numbers. With increasing functionality f, star polymers exhibit a crossover in their flow properties from those of linear polymers to a novel behavior, which resembles the tank-treading motion of elastic capsules.

DOI: 10.1103/PhysRevLett.96.188302 PACS numbers: 82.35.Lr, 47.11.Mn, 83.50.−v

The behavior of rigid and soft mesoscopic particles in shear flow is of considerable interest both from a fundamental and an applied viewpoint. Many soft matter systems, ranging from rodlike colloids to linear polymers, droplets, capsules, and vesicles have been investigated under shear-flow conditions, since this is a paradigmatic case were the dynamical behavior can be studied in a stationary nonequilibrium state [1,2]. From the technological side, flow plays an essential role in a broad spectrum of applications of soft materials, e.g., in polymer extruders, food production, and microfluidics, as well as in biological systems, e.g., blood flow. A rich dynamical behavior has been found for deformable soft objects under flow, such as tumbling, tank-treading, rupture, stretching, and collapse [3–6].

Star polymers present a special macromolecular architecture, in which several linear polymers of identical length are linked together by one of their ends to a common center. This structure is particularly interesting because it allows an almost continuous change of properties from that of a flexible linear polymer to a spherical colloidal particle with very soft pair interactions. Star polymers are therefore often called ultrasoft colloids. The properties of star polymers in and close to equilibrium have been studied intensively, both theoretically [7,8] and experimentally [9].

In this Letter, we investigate the structural and dynamical properties of a dilute solution of star polymers in shear flow—as a function of arm number f, arm length L_f, and shear rate $\dot{\gamma}$—by employing a mesoscopic simulation approach to fluid flow. The main questions we want to address are: Do stars in flow show tumbling motion with alternating collapse and stretching like linear polymers? Is there a universal scaling behavior in flow, as it has been observed for the structural and dynamical properties in equilibrium? We show that with increasing functionality f, star polymers exhibit a crossover in their flow properties from those of linear polymers to a novel behavior, which resembles those of fluid droplets or elastic capsules—with a qualitative change occurring near $f = 5$. A recent simulation study [10] of stars in shear flow was restricted to small monomer numbers, so that universal properties could not be extracted.

In order to investigate the dynamics of flexible polymers in flow, we use a hybrid simulation approach, in which standard molecular dynamics simulations for the polymer are combined with a mesoscopic simulation technique for the solvent. Consecutive monomers of a polymer chain are connected by harmonic springs with a rest length b. The excluded-volume interaction is modeled by a truncated and shifted Lennard-Jones potential with diameter σ among all the monomers. Star polymers of functionality f are modeled as f linear polymer chains of L_f monomers each, with one of their ends linked to a central particle. Linear polymers are a special case of star polymers with functionality $f = 2$. In order to account for the hydrodynamic interactions mediated by the solvent, we employ a particle-based mesoscopic simulation technique called multi-particle-collision dynamics (MPC) [11] or stochastic rotation dynamics [12]. This method consists of alternating streaming and collision steps. In the streaming step, the solvent particles of mass m move ballistically for a time h. In the collision step, particles are sorted into the cells of a cubic lattice, and their velocities relative to the center-of-mass velocity of each cell are rotated around a random axis by an angle α. This implies that mass, momentum, and energy are conserved in the collisions. A detailed description of the method can be found, e.g., in Refs. [11,13–15]. In particular, it has been shown that hydrodynamic behavior at low Reynolds and large Schmidt numbers can be described very well if the mean free path of the solvent particles is much smaller than the cell size a [15]. Finally, the interaction of the polymer with the fluid is taken into account by including the monomers in the MPC collision step [15–17]. We employ the parameters $\alpha = 130°$, $h = 0.1\sqrt{ma^2/k_BT}$, the number of particles per cell $\rho = 5$, the monomer mass $M = \rho m$, and $b = \sigma = a$. System sizes range from $(25a)^3$ to $(50a)^2 \times 150a$. The polymer dynamics in equilibrium obtained with this method has been found to agree very well with the predictions of the well-known Zimm theory [17].

Lees-Edwards boundary conditions are employed in order to impose a linear velocity profile $(v_x, v_y, v_z) = (\dot{\gamma} r_y, 0, 0)$ in the fluid in the absence of a polymer, with a tunable shear rate $\dot{\gamma}$. Particle velocities relative to the center-of-mass velocity of each cell are rescaled in each collision step in order to keep the temperature constant.

For small shear rates, the conformations of star polymers remain essentially unchanged compared to the equilibrium state. Only when the shear rate exceeds a characteristic value, which corresponds to the longest relaxation time τ of the polymer in equilibrium, a structural anisotropy as well as an alignment is induced by the flow. For star polymers, τ has been shown to be determined by the overall shape fluctuations [18]. A calculation of Zimm dynamics for the blob model of star polymers predicts $\tau \sim L_f^{3\nu} f^{1-3\nu/2}$ for large functionality [18].

A convenient quantity to characterize the structural properties and alignment of polymers in flow is the average gyration tensor, which is defined as

$$G_{\alpha\beta}(\dot{\gamma}) = \frac{1}{N_m} \sum_{i=1}^{N_m} \langle r_{i,\alpha} r_{i,\beta} \rangle, \qquad (1)$$

where $N_m = fL_f + 1$ is the total number of monomers, $r_{i,\alpha}$ is the position of monomer i relative to the polymer center of mass, and $\alpha, \beta \in \{x, y, z\}$. The average gyration tensor is directly accessible in scattering experiments. Its diagonal components, $G_{\alpha\alpha}(\dot{\gamma})$, are the squared radii of gyration of the star polymer in the α direction. In the absence of flow, the scaling behavior has been predicted [7] to be $G_{xx}(0) = G_{yy}(0) = G_{zz}(0) = R_g^2(0)/3 \sim L_f^{2\nu} f^{1-\nu}$.

The diagonal components $G_{\alpha\alpha}$ of the average gyration tensor are shown in Fig. 1 as a function of the Weissenberg number $\mathrm{Wi} = \dot{\gamma}\tau$ for various functionalities and arm lengths. These results allow several conclusions. First, we find the best data collapse for stars with different arm lengths when a scaling of the relaxation time $\tau = \tau_0 L_f^{2.0}$ is used for *all* functionalities, where $\tau_0 = \eta_s b^3/(k_B T)$ is the Zimm result for linear polymers [1], with solvent viscosity η_s, bond length b, and thermal energy $k_B T$. Remarkably, there is essentially no dependence of τ on the functionality f. Within the range of star sizes, which is currently accessible in simulations with flow, these results have to be seen as consistent with the prediction of the blob model discussed above, where $\tau \sim L_f^{1.8} f^{0.1}$ (for the Flory exponent $\nu = 0.6$). For linear polymers, a dependence $\tau \sim L_f^{2.0}$ has also been found in simulations with a solvent of Lennard-Jones particles [19]. Second, we find that the extension of a star increases with increasing shear rate in the shear direction (x), decreases in the gradient direction (y), and, for high-functionality stars, is almost independent of $\dot{\gamma}$ in the vorticity direction (z). Third, the deviation from spherical symmetry exhibits a Wi^2 power-law dependence for small shear rates for all functionalities. Such a behavior is well-known for rodlike colloids and linear polymers [1,20]. However, for stars of not too small functionality, a new scaling regime appears, where the deformation scales *linearly* with the Weissenberg number. Finally, Fig. 1 also shows that there are finite-size effects due to the finite monomer number at high shear rates.

In Fig. 2, the asphericity of star polymers—characterized by the ratio $G_1/G_3 - 1 \geq 0$ of the largest and smallest eigenvalue of the average gyration tensor—is shown as a function of the Weissenberg number for various functionalities f. Note that $G_1/G_3 - 1 = 0$ for a sphere, while it diverges in the limit of a long rod. The main result of Fig. 2 is that stars become more spherical with increasing f. In the linear scaling regime of Fig. 1, this approach to the spherical shape is found to be essentially independent of

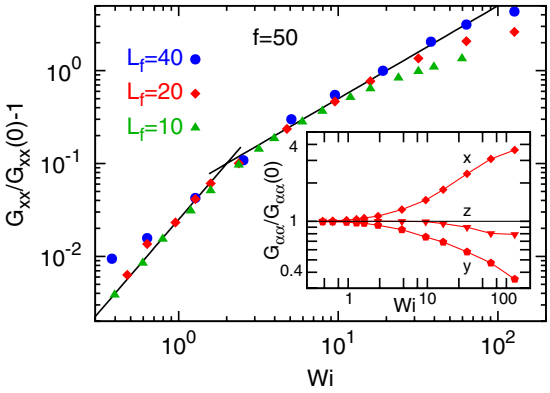

FIG. 1 (color online). Normalized component G_{xx} of the average gyration tensor as a function of the Weissenberg number $\mathrm{Wi} = \dot{\gamma}\tau$, for star polymers of $f = 50$ arms, with $L_f = 10$, 20, and 40 monomers per arm. Quadratic and linear power-law behaviors are indicated by lines. The inset shows the diagonal components of the gyration tensor (for $L_f = 20$).

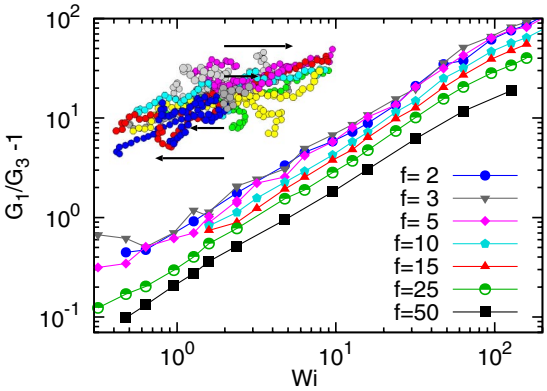

FIG. 2 (color online). Ratio of the largest (G_1) and smallest (G_3) eigenvalues of the average gyration tensor, as a function of the Weissenberg number Wi for star polymers with $L_f = 20$ monomers per arm, for various functionalities as indicated. The inset shows a typical configuration of a star with $f = 25$ and $\mathrm{Wi} = 30$ in the flow-gradient plane.

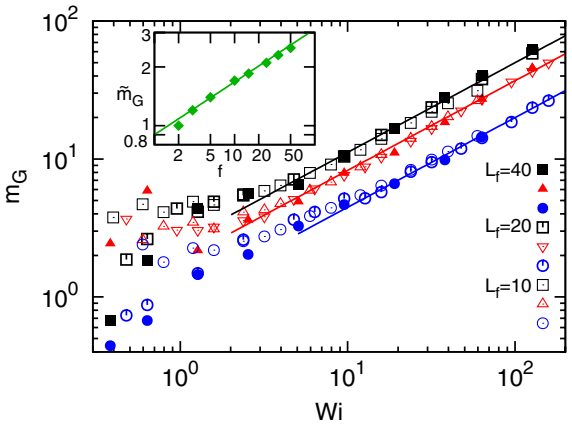

FIG. 3 (color online). Orientational resistance m_G as a function of the Weissenberg number Wi for star polymers with functionalities $f = 2$ (circles), $f = 15$ (triangles) and $f = 50$ (squares), and various arm lengths as indicated. Lines correspond to $m_G = \tilde{m}_G(f)\mathrm{Wi}^{0.65}$. The inset shows that the amplitude also follows a power law with $\tilde{m}_G(f) \sim f^{0.27}$.

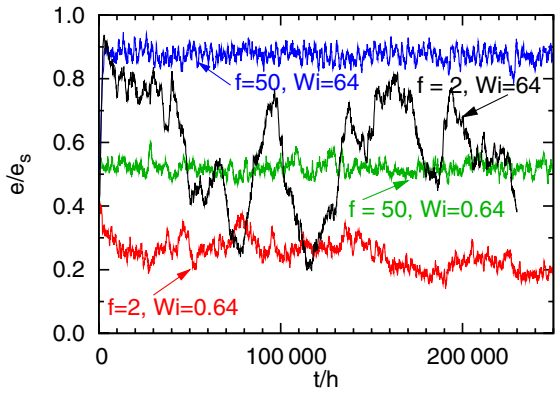

FIG. 4 (color online). Temporal evolution of the largest intramolecular distance $e = \max_{ij}|\mathbf{r}_i - \mathbf{r}_j|$ of a linear polymer and a star polymer with 50 arms, for Weissenberg numbers $\mathrm{Wi} = 0.64$ and $\mathrm{Wi} = 64$. In both cases, $L_f = 40$. The time t is measured in units of the collision time h. e_s is the length e of the fully extended star.

Weissenberg number, i.e., $G_1/G_3 - 1$ decreases by a factor which only depends on f for this range of Wi.

The average flow alignment of a (star) polymer is characterized by the orientation angle χ_G, which is the angle between the eigenvector of the gyration tensor with the largest eigenvalue and the flow direction. It can be extracted straightforwardly from the simulation data via

$$\tan(2\chi_G) = 2G_{xy}/(G_{xx} - G_{yy}) \equiv m_G/\mathrm{Wi}, \qquad (2)$$

where the right-hand side of the equation defines the orientation resistance parameter m_G [19,20]. It has been shown for several systems including rodlike colloids and linear polymers [1,20] that close to equilibrium $G_{xy} \sim \dot{\gamma}$ and $(G_{xx} - G_{yy}) \sim \dot{\gamma}^2$, hence m_G is independent of Wi. Our results for the orientation resistance are presented in Fig. 3 for star polymers of various functionalities f and arm lengths L_f. Data for different L_f collapse onto a universal curve, which approaches a plateau for small shear rates, as expected. For larger shear rates, the orientational resistance can be described by a power law $m_G(\mathrm{Wi}) \sim \mathrm{Wi}^{\mu}$. Furthermore, the amplitude can also be described by a power law (compare Fig. 3) so that

$$m_G(\mathrm{Wi}) \sim f^{\alpha}\mathrm{Wi}^{\mu} \quad \text{for } \mathrm{Wi} \gg 1, \qquad (3)$$

with $\alpha = 0.27 \pm 0.02$ and $\mu = 0.65 \pm 0.05$. For self-avoiding linear polymers, a somewhat smaller exponent $\mu = 0.54 \pm 0.03$ was obtained in Refs. [19,21]. The increase of m_G with increasing functionality (at fixed Weissenberg number) reflects the smaller asphericity of stars with larger arm number.

The data for the average orientation and deformation of a star polymer described so far seem to indicate that the properties vary smoothly and monotonically from linear polymers to star polymers of high functionality. However, this picture changes when the *dynamical behavior* is considered. It is well-known by now that linear polymers show a tumbling behavior in flow, with alternating collapsed and stretched configurations [4,5,21–23]. For large Weissenberg numbers, this leads to very large fluctuations of the largest intramolecular distance $e = \max_{ij}|\mathbf{r}_i - \mathbf{r}_j|$ in time, as demonstrated experimentally in Refs. [4,21] and reproduced in our simulations; see Fig. 4. A similar behavior is found for $f = 3$. However, for $f > 5$, a qualitatively different behavior is observed, where the overall shape and orientation depend very little on time (see Fig. 4), while the arms rotate around the center of the star [24]. Interestingly, this motion resembles the continuous tank-treading rotation observed for fluid droplets and capsules. The change in the flow properties can be seen in the distribution of the largest intramolecular distance e. Figure 5 shows that its width becomes much smaller and a *decreasing* function of

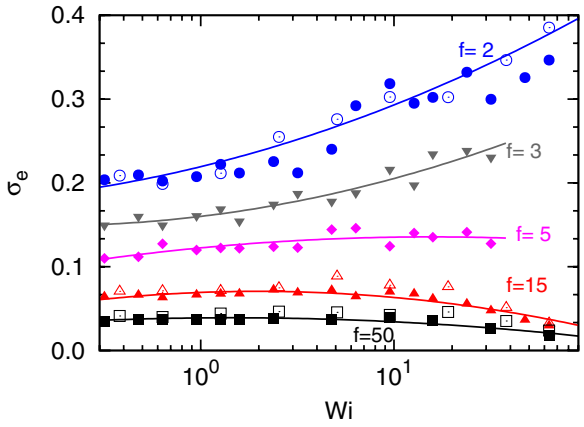

FIG. 5 (color online). Width of the distribution of the largest intramolecular distances, $\sigma_e = (\langle e^2\rangle - \langle e\rangle^2)/\langle e\rangle^2$ of a linear polymer and star polymers with up to 50 arms, as a function of the Weissenberg number Wi. Lines are guides to the eye.

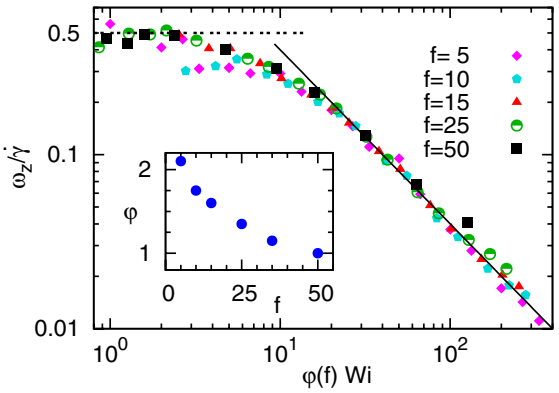

FIG. 6 (color online). Scaled rotation frequency, $\omega_z/\dot{\gamma}$, as a function of a rescaled Weissenberg number, for various functionalities as indicated. Dashed and solid lines correspond to $\omega_z/\dot{\gamma} = 1/2$ for small Wi and $\omega_z/\dot{\gamma} \sim 1/\mathrm{Wi}$ for large Wi, respectively. The inset shows the dependence of the rescaling factor φ on the arm number.

the Weissenberg number for $f > 5$. On the other hand, the behavior of a single, selected arm is qualitatively not much different from a linear polymer, as it also rotates by collapsing and stretching (see inset of Fig. 2) during the *tank-treading-like* motion [24].

In order to investigate the rotational dynamics more quantitatively, we determine the rotation frequency $\omega_\alpha = \sum_{\beta=x}^{z} \langle \Theta^{-1}_{\alpha\beta} L_\beta \rangle$ of a star, where $\Theta_{\alpha\beta} = \sum_{i=1}^{N_m} [r_i^2 \delta_{\alpha\beta} - r_{i,\alpha} r_{i,\beta}]$ is the instantaneous moment-of-inertia tensor and L_β is the instantaneous angular momentum. Since the rotation frequency for all kinds of soft objects [1,23]—like rods, linear polymers, droplets, and capsules—depends linearly on $\dot{\gamma}$ for small shear rates, we plot in Fig. 6 the reduced rotation frequency $\omega_z/\dot{\gamma}$ as a function of the Weissenberg number. The data approach $\omega_z/\dot{\gamma} = 1/2$ for small Wi, as expected. For larger shear rates, the reduced frequency decreases due to the deformation and alignment of the polymers in the flow field. With increasing arm number, the reduction of $\omega_z/\dot{\gamma}$ at a given Weissenberg number becomes smaller, since the deviation from the spherical shape decreases. Remarkably, we find that the frequency curves for all stars with $f > 5$ collapse onto a universal scaling function, when $\omega_z/\dot{\gamma}$ is plotted as a function of a rescaled Weissenberg number; see Fig. 6. For high shear rates, $\omega_z/\dot{\gamma}$ decays as Wi^{-1}, which implies that the rotation frequency becomes *independent* of $\dot{\gamma}$. A similar behavior has been observed for capsules at high shear rates [25].

In summary, we have shown by mesoscale simulations that star polymers in shear flow show a very rich structural and dynamical behavior. With increasing functionality, stars in flow change from linear-polymer-like to capsule-like behavior. These macromolecules are therefore interesting candidates to tune the viscoelastic properties of complex fluids.

We thank H. Noguchi, J. Stellbrink, J. K. G. Dhont, D. Vlassopoulos, and M. P. Lettinga for valuable discussions. Financial support by the German Research Foundation (DFG) within SFB TR6, and the European Network of Excellence "SoftComp" (Contract No. NMP3-CT-2004-502235) is gratefully acknowledged. M. R. also thanks the Spanish MCYT (project No. FIS2004-01934) for partial support.

*Email address: m.ripoll@fz-juelich.de

[1] M. Doi and S. F. Edwards, *The Theory of Polymer Dynamics* (Oxford University Press, Oxford, 1986).
[2] R. G. Larson, *The Structure and Rheology of Complex Fluids* (Oxford University Press, New York, 1999).
[3] H. A. Stone, Annu. Rev. Fluid Mech. **26**, 65 (1994).
[4] D. E. Smith, H. P. Babcock, and S. Chu, Science **283**, 1724 (1999).
[5] P. LeDuc, C. Haber, G. Bao, and D. Wirtz, Nature (London) **399**, 564 (1999).
[6] S. Gerashchenko and V. Steinberg, Phys. Rev. Lett. **96**, 038304 (2006).
[7] G. S. Grest, K. Kremer, and T. A. Witten, Macromolecules **20**, 1376 (1987).
[8] C. N. Likos, Phys. Rep. **348**, 267 (2001).
[9] D. Vlassopoulos, G. Fytas, T. Pakula, and J. Roovers, J. Phys. Condens. Matter **13**, R855 (2001).
[10] J. G. Hernández Cifre, R. Pamies, M. C. López Martínez, and J. García de la Torre, Polymer **46**, 6756 (2005).
[11] A. Malevanets and R. Kapral, J. Chem. Phys. **110**, 8605 (1999); **112**, 7260 (2000).
[12] T. Ihle and D. M. Kroll, Phys. Rev. E **63**, 020201(R) (2001).
[13] N. Kikuchi, C. M. Pooley, J. F. Ryder, and J. M. Yeomans, J. Chem. Phys. **119**, 6388 (2003).
[14] E. Tüzel, M. Strauss, T. Ihle, and D. M. Kroll, Phys. Rev. E **68**, 036701 (2003).
[15] M. Ripoll, K. Mussawisade, R. G. Winkler, and G. Gompper, Europhys. Lett. **68**, 106 (2004); Phys. Rev. E **72**, 016701 (2005).
[16] A. Malevanets and J. M. Yeomans, Europhys. Lett. **52**, 231 (2000).
[17] K. Mussawisade, M. Ripoll, R. G. Winkler, and G. Gompper, J. Chem. Phys. **123**, 144905 (2005).
[18] G. S. Grest, K. Kremer, S. T. Milner, and T. A. Witten, Macromolecules **22**, 1904 (1989).
[19] C. Aust, M. Köger, and S. Hess, Macromolecules **32**, 5660 (1999).
[20] A. Link and J. Springer, Macromolecules **26**, 464 (1993).
[21] R. E. Teixeira, H. P. Babcock, E. S. G. Shaqfeh, and S. Chu, Macromolecules **38**, 581 (2005).
[22] P. G. de Gennes, J. Chem. Phys. **60**, 5030 (1974).
[23] C. Aust, S. Hess, and M. Köger, Macromolecules **35**, 8621 (2002).
[24] See EPAPS Document No. E-PRLTAO-96-062620 for animation of the dynamics of a star with $f = 25$ and $\mathrm{Wi} = 30$. For more information on EPAPS, see http://www.aip.org/pubservs/epaps.html.
[25] Y. Navot, Phys. Fluids **10**, 1819 (1998).